Published in final edited form as:
Free Radic Biol Med. 2010 November 30; 49(10): . doi:10.1016/j.freeradbiomed.2010.08.018.

SOD1 and MitoTEMPO partially prevent MPTP, necrosis and mitochondrial apoptosis following ATP depletion-recovery

Huan Ling Liang[1,2], **Filip Sedlic**[3], **Zeljko Bosnjak**[3], and **Vani Nilakantan**[1,2]

[1]Division of Transplant Surgery, Medical College of Wisconsin, Milwaukee, WI 53226

[2]Kidney Disease Center, Medical College of Wisconsin, Milwaukee, WI 53226

[3]Departments of Anesthesiology and Physiology, Medical College of Wisconsin, Milwaukee, WI 53226

Abstract

Generation of excessive reactive oxygen species (ROS) leads to mitochondrial dysfunction, apoptosis and necrosis in renal ischemia-reperfusion (IR) injury. Previously we showed that lentiviral vector mediated over-expression of superoxide dismutase-1 (SOD1) in proximal tubular epithelial cells (LLC-PK_1) reduced cytotoxicity in an *in vitro* model of IR injury. Here, we examined the effects of SOD1 over-expression on mitochondrial signaling following ATP depletion-recovery (ATP-DR). To examine the role of mitochondrial ROS, a subset of cells were treated with the mitochondrial antioxidant, MitoTEMPO. ATP-DR-mediated increases in mitochondrial calcium ($[Ca^{2+}]_m$), loss of mitochondrial membrane potential ($\Delta\Psi_m$) and increase in mitochondrial permeability transition pore (MPTP) were attenuated by SOD1 and MitoTEMPO ($P < 0.01$). SOD1 prevented ATP-DR induced mitochondrial Bax translocation, although the release of pro-apoptotic proteins from mitochondria was not prevented by SOD1 alone and required the presence of both SOD1 and MitoTEMPO. SOD1 suppressed the increase in c-jun phosphorylation suggesting that JNK signaling regulates Bax translocation to mitochondria via ROS. ATP-DR-mediated changes in MPTP and mitochondrial signaling increased necrosis and apoptosis, both of which were partially attenuated by SOD1 and MitoTEMPO. These studies show that SOD1 and MitoTEMPO preserve mitochondrial integrity and attenuate ATP-DR mediated necrosis and apoptosis.

Keywords

ATP depletion; mitochondrial membrane potential; calcium; cytochrome c; Bax; SOD1

Introduction

Renal ischemia reperfusion (IR) injury, one of the common causes of acute kidney injury induces severe cytotoxicity in the outer medullary proximal tubules. IR substantially alters the function of renal epithelial cells, which includes decrease in cellular ATP, increase in calcium, oxidative stress, membrane lipid peroxidation, enzyme dysfunction and impairment of intracellular antioxidant defenses, particularly superoxide dismutase-1 (SOD1) [1–4] rendering the cell more susceptible to oxidative stress [5]. Oxidative stress and the generation of reactive oxygen species (ROS) are believed to be one of the major mediators of injury during renal IR [6–8]. Therefore, the survival or death of the renal epithelial cell

Corresponding author: Vani Nilakantan, Ph.D., Division of Transplant Surgery, Kidney Disease Center, H4135, Medical College of Wisconsin, 8701 Watertown Plank Rd, Milwaukee, WI 53226., Tel: 414-456-4819, Fax: 414-456-6312, vnilakan@mcw.edu.

will in part, depend on the balance between the ROS generation and their removal by the intracellular antioxidant systems, such as SOD, catalase and glutathione peroxidase. Of the three isoforms of SOD, SOD1 is the most abundant in the kidney and thus serves as a major antioxidant system in disproportionating $O_2^{\bullet -}$ into oxygen and H_2O_2 which is further detoxified by glutathione peroxidase or catalase [9]. Deficiency of SOD1 increases susceptibility to IR-induced acute kidney injury in mice, and the adenoviral transfer of SOD1 attenuates IR injury in the kidney [10]. SOD2 is located exclusively in mitochondrial matrix, and over-expression of SOD2 has shown protective effects in various cardiac injury models [11–13]. However, the exact molecular mechanism and signaling pathways of SODs in renal proximal tubular cells are still not very clear.

Mitochondria play an important role in many cellular processes including production of ATP, fatty acid oxidation, control of apoptosis and necrosis, and regulation of cytosolic Ca^{2+} homeostasis [14–16]. Mitochondria are the primary site of ROS production and also a target for oxidative stress. The mitochondrial permeability transition pore (MPTP) is a nonspecific channel formed by components from the inner mitochondrial membrane and its opening initiates cell death. The occurrence of a sudden change in the permeability of the mitochondrial membranes due to MPTP opening is usually induced by oxidative stress and mitochondrial calcium ($[Ca^{2+}]_m$) overload causing an arrest in mitochondrial respiration and leading to necrotic or apoptotic cell death [17, 18]. Cell death can also occur after the translocation of the pro-apoptotic protein Bax to the outer mitochondrial membrane, which activates apoptosis via the release of mitochondrial proteins, such as cytochrome *c* or Smac/Diablo.

Previously, we have shown that the over-expression of SOD1 partially reduced cytotoxicity and prevented caspase-3 activation in ischemic renal epithelial cells [19]. However, the role of the SOD1 on mitochondrial signaling in ischemic injury and the importance of ROS scavenging in cytosol vs. mitochondria is still unclear. The current study was thus undertaken to determine the effects of SOD1 and MitoTEMPO, a mitochondria-targeted antioxidant, on mitochondrial function and signaling pathways in an *in vitro* ATP depletion-recovery (ATP-DR) injury model. Our findings indicate that the over-expression of SOD1 and MitoTEMPO treatment in proximal tubular epithelial cells prevent $[Ca^{2+}]_m$ overload, attenuate MPTP opening and partially block the mitochondrial translocation of the pro-apoptotic protein Bax following ATP-DR thus attenuating both necrotic and apoptotic pathways.

Material and methods

Cell culture

LLC-PK_1 (a porcine proximal tubular epithelial cell line) was obtained from the American Type Culture Collection (Rockville, MD) and grown in α-MEM containing 10% fetal bovine serum (Invitrogen, Carlsbad, CA) at 37°C in a 5% CO_2 with 95% air humidified incubator. The SOD1 (LLC-SOD1) or EGFP (LLC-EGFP) over-expressing LLC-PK_1 cells have been produced using lentiviral vector mediated transduction and have been characterized by our laboratory in a previous study [19]. Both LLC-EGFP and LLC-SOD1 cells were grown to confluence before initiation of the ATP-DR injury.

ATP-DR protocols

ATP-DR protocols were performed as previously reported [20, 21]. In brief, both LLC-EGFP and LLC-SOD1 cells were grown in α-MEM containing 10% FBS before initiation of the ATP-DR. Cells were washed with Dulbecco's phosphate buffered saline (DPBS) and incubated with prewarmed serum-free α-MEM 30 min prior to ATP depletion. ATP

depletion was induced by substrate deprivation and the addition of 0.1 μM antimycin A, a complex III inhibitor, for 0.5, 1, or 2 hours. Following the various ATP depletion time points, the cells were recovered in serum-free α-MEM for periods ranging from 5 minutes to 1 hour (DR, 30 min-5 min, 1h-15 min, 1h-1h, 2h-30 min or 2h-1h). At the end of the experiment, data was collected using laser-scanning confocal microscopy or harvested for mitochondrial isolation and western blot analysis. Control cells (SF) were grown in parallel and underwent equivalent washes and incubated in serum-free (SF) α-MEM throughout the experiment.

MitoTEMPO treatment

A subset of wild type LLC-PK_1, LLC-EGFP and LLC-SOD1 cells was treated with 1 nM of the mitochondria-targeted antioxidant MitoTEMPO during the ATP-DR. At the end of the experiment, cells were used for various analyses.

SOD activity assay

SOD activity was measured using a commercially available superoxide dismutase assay kit (Cayman Chemical, Ann Arbor, MI). This kit relies on tetrazolium salt based detection of superoxide radicals generated by xanthine oxidase. To assess for SOD2 activity, 2 mM potassium cyanide was added to inhibit SOD1 and SOD3 activity. The absorbance was read at 450 nm according to manufacturer's instructions.

ATP measurement

ATP was measured in the cell extracts using a commercially available luminescence based assay (Invitrogen, Carlsbad, CA) in a Modulus luminometer (Promega, Madison, WI). Briefly, cells were grown to confluence in 6 well plates and underwent ATP depletion for 2 hours followed by recovery for 1 hour. The cells were lysed and ATP levels were measured according to manufacturer's instructions and presented as percent of control.

$[Ca^{2+}]_m$ and mitoTracker staining in LLC-PK_1 cells

$[Ca^{2+}]_m$ was first tested in wide type LLC-PK_1 cells and monitored using rhod-2 AM (4 μM; Invitrogen) that was selectively loaded into mitochondria using modification of previously described cold-warm loading protocol [22]. In brief, rhod-2 AM was loaded into LLC-PK_1 cells (which were subject to ATP-DR) first at the lower, room temperature for 30 min, then for additional 10 min at 37°C, followed by dye washout at 37°C for additional 1 h. This protocol enables selective loading of rhod-2 AM into mitochondria and removal of residual dye from the cytosol. To verify the mitochondrial localization of rhod-2 signal, MitoTracker Green (1 μM, Invitrogen), a mitochondrial targeted probe was loaded during last 15 minutes of incubation with the rhod-2 AM. The fluorescence signal of both dyes co-localized and exhibited specific mitochondrial pattern, confirming mitochondrial localization of rhod-2 signal. Rhod-2 AM was excited using a green HeNe laser at 543 nm and emitted fluorescence was collected at 590/40 nm. Measurements of $[Ca^{2+}]_m$ uptake in LLC-EGFP and LLC- SOD1 cells with or without MitoTEMPO were conducted following 1h-1h ATP-DR protocol.

Laser-scanning confocal microscopy

$[Ca^{2+}]_m$ and mitochondrial membrane potential ($\Delta\Psi_m$) in LLC-EGFP and LLC-SOD1 cells was monitored using laser-scanning confocal microscope (Eclipse TE2000-U; Nikon, Tokyo, Japan) with a 60xA/1.40 oil-immersion objective (Nikon). MetaMorph 6.1 software (Universal Imaging, West Chester, PA) was used for data analysis. Fluorescence intensities are expressed as arbitrary units (a.u.).

Measurements of $\Delta\Psi_m$ by TMRE and JC-1

LLC-EGFP and LLC- SOD1 cells underwent 1h-1h ATP-DR and were loaded with 50 nM tetra-methyl rhodamine ethyl ester (TMRE) during the last 15 min of ATP-DR, and visualized using confocal microscopy. TMRE is a lipophilic, potentiometric dye that is driven into mitochondria by $\Delta\Psi_m$. Green HeNe laser was used to excite TMRE at 543 nm, followed by fluorescence collection at 590/40 nm.

JC-1 selectively enters mitochondria driven by $\Delta\Psi_m$ and reversibly changes color from green to red as the membrane potential increases. In healthy cells with high mitochondrial $\Delta\Psi_{m,}$ JC-1 spontaneously forms complexes known as J-aggregates with intense red fluorescence. On the other hand, in unhealthy cells with low $\Delta\Psi_{m,}$ JC-1 remains in the monomeric form, which shows only green fluorescence. To avoid the signal interference between EGFP and JC-1 we used LLC-PK_1 instead of EGFP cells. LLC-PK_1 and LLC-SOD1 cells were grown in a 24-well culture plate at a density of 1×10^5 cells/ml. After 1h-1h of the ATP-DR protocols, JC-1 (Cayman Chemical, Ann Arbor, MI) was loaded at a dilution of 1:15 in α-MEM and incubated at 37°C for 20 minutes. After washing once with pre-warmed JC-1 assay buffer, images were directly taken by using an Olympus IX50 inverted microscope (Olympus America, Center Valley, PA) or microplate was read in a fluorometer with excitation/emission settings at 560/595 nm and 485/535 nm. The intensity of green and red fluorescence was also quantified using ImageJ software (NIH), and data are presented as mean of red/green fluorescence ratio.

Mitochondrial isolation

After varying time points of ATP-DR, the cells were harvested in cold DPBS, centrifuged for 3 minutes at 2000 rpm at 4°C, and cell pellet was re-suspended in ice-cold mitochondrial isolation buffer (250 mM sucrose, 20 mM HEPES, 10 mM KCl, 1.0 mM EDTA, 1.5 mM $MgCl_2$) with protease inhibitors, and incubated for 30 minutes on ice. The cell membrane was lysed by drawing the mixture in and out the insulin syringe for total 20 times on ice followed by centrifugation for 15 minutes at 750 g at 4°C. The cytosolic and mitochondrial fractions were separated by centrifuging supernatant at 12, 000 g for 15 minutes at 4°C. The mitochondrial pellet was washed three times with mitochondrial isolation buffer and mitochondrial pellet was re-suspended in RIPA buffer and stored at −80°C until assay. Protein concentration was measured using a protein assay kit from Bio-Rad (Hercules, CA). To test the purity of the mitochondria, western blots were used to determine the presence of GAPDH and the absence of cytochrome c oxidase in the cytosolic fraction and the absence of GAPDH and the presence of cytochrome c oxidase in the mitochondrial fraction.

Western blots

Twenty five micrograms of whole cell lysate, mitochondrial or cytosol fraction from LLC-PK_1, LLC-EGFP and LLC-SOD1 treated cells were run on 15% or 4–20% creatinine gel and transferred to polyvinylidene fluoride (PVDF) membrane. These fractions were electrophoresed on the same gel to avoid any gel to gel variations and stained with Ponceau S to ensure equal protein loading. After blocking 1 hour at room temperature (RT), the blots were incubated with one of the following primary antibodies: Bax (Santa Cruz Biotechnology, Santa Cruz, CA, 1:200); Bcl-2 (Santa Cruz Biotechnology, Santa Cruz, CA, 1:1000); cytochrome *c* (BD biosciences, San Jose, CA, 1:1000); cytochrome *c* oxidase subunit I (Invitrogen, Carlsbad, CA, 1:1000); GADPH (Chemicon, Temecula CA, 1:2000); phosphoSAPK/JNK (Cell Signaling Technology, Inc. Danevers, MA, 1:1000); total SAPK/JNK (Cell Signaling Technology, Inc. Danevers, MA, 1:1000); phospho-c-Jun (Cell Signaling Technology, Inc. Danvers, MA, 1:1000) and Smac/Diablo (AbCam, Cambridge, MA, 1:1000) overnight at 4°C. After washing, the membranes were probed with secondary

goat-anti-rabbit, or goat-anti-mouse IgG conjugated to horseradish peroxidase (Bio-Rad) at 1:10,000 for 1 hour at RT. The blots were visualized with ECL.

Apoptosis and necrosis

Cells were evaluated for necrosis and apoptosis by Annexin V-FITC (5 μg/ml; BD Bioscience Pharmingen) and propidium iodide (5 μg/ml; BD Pharmingen, Franklin Lakes, NJ) staining, respectively, according to manufacturer's instructions. Briefly, for microscopic visualization, cells were grown on coverslips coated with poly-L-lysine (Sigma, St. Louis MO). After 2h–1h ATP-DR with or without MitoTEMPO treatment, coverslips were removed from the culture dish and washed with DPBS, then stained with propidium iodide and Annexin V in 1x Binding buffer for 15 min at room temperature in the dark. After washing with DPBS, the coverslips were mounted on glass slides using Gel/mount (Electron Microscopy Science) and imaged under a Nikon fluorescence microscope. Annexin V positive cells were classified as apoptotic, and propidium positive cells were considered as necrotic. Fluorescence was analyzed using ImageJ software and the number of propidium positive cells per field was counted in randomly selected areas.

Statistical analysis

Data are expressed as mean values ± SEM. The significance of differences in mean values was evaluated by one-way ANOVA, followed by a Newman-Keuls multiple comparison test. $P < 0.05$ was considered statistically significant.

Results

ATP levels

To determine whether SOD1 or MitoTEMPO had an effect on ATP levels, we measured ATP in EGFP, SOD1 and MitoTEMPO treated cells following 2h-1h ATP-DR. ATP levels were 39 ± 4.08 % higher in the SOD1 over-expressing cells compared to EGFP cells under serum free conditions. Following ATP-DR, ATP levels were decreased to 77 ± 5.29 % and 80 ± 0.36 % of control in the EGFP and SOD1 cells respectively. MitoTEMPO treatment did not restore ATP levels in the EGFP cells (76 ± 9.17 %) and had a slight tendency to improve ATP levels in the SOD cells (86 ± 4.95 %).

SOD activity

SOD activity was measured in EGFP, SOD1 and MitoTEMPO treated cells under serum free and ATP depleted conditions. MitoTEMPO did not affect total SOD activity in either EGFP or SOD1 cells (data not shown). However, there was a significant decrease in SOD2 activity in the EGFP cells following 2h-1h ATP-DR and MitoTEMPO partially restored SOD2 activity (Fig 1A). Surprisingly, in the SOD1 over-expressing cells, SOD2 activity was higher compared to EGFP cells under serum free conditions (Fig 1A). Following ATP-DR, the SOD2 activity was preserved in the SOD1 over-expressing cells and MitoTEMPO did not have a significant effect (Fig 1A).

DHE fluorescent microscopic imaging was used to evaluate the superoxide levels in EGFP, SOD1 and MitoTEMPO cells. Following ATP-DR, there was an increase in DHE staining in EGFP cells (Fig 1B) and this was partially attenuated in the SOD1 cells. The addition of MitoTEMPO to EGFP and SOD1 cells further decreased DHE fluorescent staining following ATP-DR (Fig 1B).

Co-localization of rhod-2 AM and MitoTracker

To verify selective loading of rhod-2 into mitochondria, LLC-PK_1 cells were ATP depleted and incubated with the Mitotracker Green along with rhod-2 AM. As shown in Fig 2A, the rhod-2 fluorescence co-localized with Mitotracker Green and exhibited characteristic mitochondrial pattern, indicating the preferential mitochondrial loading of rhod-2 AM.

ATP-DR induces $[Ca^{2+}]_m$ overload

LLC-PK_1 cells were used to test the time-dependant effects of the ATP depletion and-recovery phases on the increase in $[Ca^{2+}]_m$. Initial experiments indicated that there was a significant increase in $[Ca^{2+}]_m$ within 1 hour of ATP depletion (data not shown). Following 1 h of ATP depletion, the rhod-2 fluorescence increased progressively during the recovery period and reached a peak at about 90 minutes ($P<0.05$) , indicating time-dependant accumulation of mitochondrial Ca^{2+} (Fig. 2B). Treatment with the calcium ionophore, ionomycin increased the rhod-2 fluorescence intensity, which was blocked with the putative inhibitor of mitochondrial Ca^{2+} uniporter, ruthenium red, corroborating that rhod-2 primarily reports changes in $[Ca^{2+}]_m$($P < 0.01–0.001$) (Fig. 2B).

SOD1 over-expression and MitoTEMPO partially prevent $[Ca^{2+}]_m$ accumulation following ATP-DR

To assess the potential role of SOD1 in ATP-DR-induced $[Ca^{2+}]_m$ overload, we compared $[Ca^{2+}]_m$ in LLC-SOD1 and LLC-EGFP cells following ATP-DR. In addition, we also tested the effect of mitochondrial ROS scavenging using MitoTEMPO. ATP-DR induced a significant increase in rhod-2 fluorescence intensity, an index of increase in $[Ca^{2+}]_m$, indicating that $[Ca^{2+}]_m$ overload was a consequence of increased ROS production induced by ATP-DR (Fig 2C) ($P < 0.05$). Similarly, the treatment with the mitochondria targeted antioxidant MitoTEMPO also partially blocked the increase in $[Ca^{2+}]_m$ although to a lesser extent than SOD1 ($P < 0.05$) (Fig. 1C). In combination, MitoTEMPO and SOD1 exhibited a small additive effect and further attenuated ATP-DR mediated increase in $[Ca^{2+}]_m$ ($P< 0.05$) (Fig 2C).

SOD1 over-expression and MitoTEMPO partially prevent the loss of $\Delta\Psi_m$ due to MPTP opening following ATP-DR

Excessive ROS production together with the $[Ca^{2+}]_m$ can cause the sustained opening of the MPTP leading to apoptosis and/or necrosis [23–26]. Since MPTP causes the collapse of the $\Delta\Psi_m$, we assessed the changes in the $\Delta\Psi_m$ following 1h-1h ATP-DR. In LLC-EGFP cells ATP-DR induced the collapse of the $\Delta\Psi_m$, observed as a substantial decrease in TMRE fluorescence (Fig 3). In the presence of MPTP blockers cyclosporine A (CsA) and bongkrekic acid (BA) the loss TMRE fluorescence was attenuated, indicating that MPTP opening was in part responsible for the observed collapse of $\Delta\Psi_m$ (Fig 3, $P< 0.001$). In LLC-SOD1 cells or cells treated with MitoTEMPO, the $\Delta\Psi_m$ collapse was also prevented, suggested that cytosolic or mitochondrial ROS scavenging inhibited MPTP and attenuated ATP-DR induced mitochondrial depolarization (Fig 3, $P< 0.001$). In combination, SOD1 over-expression and MitoTEMPO exhibited small, but not significant additive effect (Fig 3).

We also used JC-1, another indicator of $\Delta\Psi_m$ to verify the results obtained using TMRE. In agreement with the results above, ATP-DR caused mitochondrial depolarization, which was attenuated by SOD1 (Fig. 4, $P< 0.05$). MitoTEMPO treatment also showed tendency to attenuate the loss of $\Delta\Psi_m$, but this did not reach statistical significance.

Effects of SOD1 over-expression and MitoTEMPO on Bax mitochondrial translocation

Bax translocation to the mitochondria is a key event regulating the release of proteins such as cytochrome c and Smac/Diablo from the mitochondria leading to downstream apoptotic events [27]. To determine whether SOD1 also had an effect on the translocation of pro- and antiapoptotic genes, Bax and Bcl-2 to the mitochondria, mitochondrial fractions were isolated from both LLC-EGFP and LLC-SOD1 after 1h-1h ATP-DR, and levels of Bax and Bcl-2 were determined. Over-expression of SOD1 partially prevented Bax translocation to mitochondria compared to LLC-EGFP cells ($P < 0.05$) (Fig. 5A and B), but did not alter Bcl-2 expression after 1h-1h ATP-DR (data not shown). Addition of MitoTEMPO alone in the LLC-EGFP cells had a tendency to decrease Bax translocation to the mitochondria but when used in conjunction with SOD1, it slightly increased mitochondrial Bax translocation (Fig. 5A–D).

Effect of SOD1 on cytochrome c release from mitochondria following ATP-DR

To evaluate the effect of SOD1 on the release of pro-apoptotic proteins from mitochondria such as cytochrome *c* in ATP-DR, the levels of cytochrome *c* were determined by western blotting in mitochondrial and cytosolic fractions. Cytochrome *c* release from mitochondria is presented as ratio of cytochrome *c* levels in cytosol and mitochondria in both LLC-EGFP and LLC-SOD1 cells after 1h-1h or 2h-1h ATP-DR (Fig. 6A and B). In the early phase of ATP depletion-recovery injury (1h-1h), SOD1 over-expression or MitoTEMPO treatment had no effect on cytochrome *c* release (Fig. 6A). At the later time point (2h-1h), SOD1 by itself did not prevent cytochrome *c* release, however, in conjunction with MitoTEMPO, the release of cytochrome *c* from mitochondria was partially prevented (Fig. 6B).

Effect of SOD1 and MitoTEMPO on Smac/Diablo release from mitochondria following ATP-DR

We next examined the effects of SOD1 on the release of other mitochondrial proteins such as Smac/Diablo following ATP-DR. Smac/Diablo from mitochondrial and cytosol fraction was further evaluated by western blots following 1h-1h and 2h-1h ATP-DR. Changes in Smac/Diablo are presented as ratio of cytosol to mitochondrial protein levels in both LLC-EGFP and LLC-SOD1 cells (Fig. 6C and D). SOD1 over-expression alone tended to increase Smac/Diablo release at the early time point and did not affect the release of Smac/Diablo at the late time point (Fig 6C and D). However the addition of MitoTEMPO prevented the release of Smac/Diablo into the cytosol at both time points (Fig 6C and D).

Effect of SOD on SAPK/JNK phosphorylation following ATP-DR

JNK has been shown to promote Bax translocation to mitochondria by phosphorylation of 14-3-3 proteins [28] which in turn induce release of pro-apoptotic proteins such as Smac/Diablo from the mitochondria. To further determine whether the effects of SOD1 on Bax translocation are dependant on SAPK/JNK, the phosphorylation of JNK was tested in total cell lysates from LLC-EGFP and LLC-SOD1 cells following the different time points of ATP-DR. There was no phosphorylation of SAPK/JNK following the very early phases of ATP depletion (30 minutes) (Fig. 7A). However, SAPK/JNK phosphorylation was initiated at 1h ATP depletion and within 15 minutes of the recovery period, and this was sustained until 2 hours of ATP depletion (Fig. 7B and C). SOD1 over-expression had a tendency to prevent SAPK/JNK phosphorylation at both the 1 hour and 2 hour time points of ischemia (Fig. 7B and C). Interestingly, MitoTEMPO did not prevent SAPK/JNK phosphorylation in any of the time points tested (Fig. 7A–C).

SOD1 decreases c-Jun phosphorylation following ATP-DR

To test whether SOD1 or MitoTEMPO have effects on nuclear protein expression downstream of SAPK/JNK, the level of phospho-c-Jun was measured by western blot from total cell lysates following 1h-15 min ATP-DR. To test the interaction between SOD1 and JNK in the activation of c-Jun, a specific JNK inhibitor, JNK-1, was included. We did not observe c-Jun phosphorylation under control conditions, but SOD1 attenuated c-Jun phosphorylation following ATP-DR injury with or without MitoTEMPO compared to LLC-EGFP cells (Fig. 7D). JNK-1 partially prevented c-Jun phosphorylation in both LLC-EGFP and LLC-SOD1 cells (Fig. 7D).

SOD1 and MitoTEMPO decreased necrosis and apoptosis following ATP-DR

To test the effects of SOD1 on apoptosis and necrosis, the percentage of Annexin V positive and propidium positive cells was measured in control and cell subject to ATP-DR cells. SOD1 and MitoTEMPO significantly reduced both Annexin V fluorescence and the number of propidium positive cells following 2h-1h ATP-DR compared to control ($P < 0.05–0.001$) (Fig. 8).

Discussion

The present study documents the effects of SOD1 over-expression and MitoTEMPO treatment on preservation of mitochondrial integrity in an *in vitro* model of ATP-DR. The main findings of this study were the following: 1) $[Ca^{2+}]_m$ increases progressively with the recovery time which is accompanied by a loss of $\Delta\Psi_m$, in part mediated by MPTP opening; 2) SOD1 over-expression partially prevents $[Ca_{2+}]_m$ overload and attenuates MPTP opening; 3) SOD1 inhibits Bax translocation to mitochondria and partially attenuates c-Jun phosphorylation following ATP-DR; 4) the mitochondria targeted antioxidant, MitoTEMPO is also effective in attenuating $[Ca^{2+}]_m$ overload, loss of $\Delta\Psi_m$ and MPTP opening and prevents Smac/Diablo release without affecting SAPK/JNK phosphorylation.

$[Ca^{2+}]_m$ overload combined with other factors is one of the primary triggers leading to the release of pro-apoptotic proteins from the mitochondria [15, 25, 29]. Our result indicating an increase in $[Ca^{2+}]_m$ in the early stages of ATP-DR is consistent with a previous report demonstrating that there is a significant increase in $[Ca^{2+}]_m$ within 1 hour of reperfusion which is elevated up to 24 hours post reperfusion and correlates with decreased mitochondrial respiration and renal function in a model of renal IR injury [30]. To our knowledge, our study is the first to show that over-expression of SOD1 and MitoTEMPO treatment can prevent ATP-DR-induced increases in $[Ca^{2+}]_m$, although other investigators have shown an increase in intracellular Ca^{2+} signaling and mitochondrial depolarization in mutant SOD1 mouse models of amyotrophic lateral sclerosis[31, 32]. Our result is further supported by the phenomenon of ROS-induced Ca^{2+} release [33] where ROS/oxidative stress stimulate Ca^{2+} release from the endoplasmic reticulum, and also inhibit intracellular Ca^{2+} pumps, thereby inhibiting its clearance from the cytosol.

The maintenance of the $\Delta\Psi_m$ is important for normal mitochondrial function, and its loss via opening of the MPTP leads to initiation of necrotic and apoptotic pathways [26, 34]. In our study, ATP depletion-recovery injury induced a dramatic loss of the $\Delta\Psi_m$ evaluated by both TMRE and JC-1 in LLC-EGFP or LLC- PK_1 cells. The collapse of $\Delta\Psi_m$ was attenuated by MPTP inhibition, indicating that in part MPTP is responsible for the observed mitochondrial depolarization. The collapse of $\Delta\Psi_m$ was also prevented by SOD1 over-expression and MitoTEMPO treatment suggesting that ROS scavenging blocked MPTP. This effect was caused either directly by decreasing ROS, a major MPTP trigger [35], and/or indirectly by

attenuating ROS-induced Ca^{2+} release [33] and $[Ca^{2+}]_m$ accumulation, another MPTP trigger.

MPTP can lead to both necrosis and apoptosis depending on whether the injury is transient or sustained. In our study, the ATP depletion mediated increase in necrosis (propidium iodide) and apoptosis (annexin V) was attenuated by both SOD1 and MitoTEMPO. This was consistent with our previous finding that over-expression of SOD1 partially reduces apoptosis by preventing caspase 3 activation [19] and with previous reports showing that over-expression of the mitochondrial SOD2 protects against injury mediated cell death [12, 13, 36]. Similar to the effects of MitoTEMPO on our model of injury, another mitochondria-targeted antioxidant, MitoQ also prevents cardiac dysfunction by attenuating mitochondrial oxidative damage or mitochondrial ROS generation in astrocytes [37–40].

During the apoptotic process, several key events occur in mitochondria, including the release of caspase activators such as cytochrome *c*, Smac/Diablo and $HtrA_2$, which is accompanied by changes in electron transport chain, and loss of $\Delta\Psi_m$ [41]. Bax translocation to the mitochondria is a major trigger that compromises the mitochondrial membrane and allows for the release of pro-apoptotic proteins and initiation of apoptosis [42]. It has also been suggested that Bax can elicit pro-apoptotic signaling from the mitochondria independent of MPTP [43, 44]. In our study, SOD1 was able to partially prevent Bax translocation to the mitochondria although it was not able to attenuate cytochrome *c* or Smac/Diablo release by itself. Nevertheless, when used in conjunction with MitoTEMPO, SOD1 prevented the release of cytochrome c and Smac/Diablo. Previous studies using a model of neuronal ischemia have shown that SOD1 over-expression in transgenic mice can prevent early cytochrome *c* and Smac/Diablo release and prevent DNA fragmentation after transient ischemia [45–47]. In contrast to these studies, our results indicate that scavenging of cytosolic ROS by SOD1 alone was insufficient to prevent the release of cytochrome c and Smac/Diablo and additional scavenging of mitochondrial ROS (by MitoTEMPO) was required to prevent the release of pro-apoptotic proteins from the mitochondria following ATP-DR.

JNK signaling has been shown to be involved in ROS-mediated apoptosis [48–51] facilitating the mitochondrial translocation of Bax. Increased phosphorylation of JNK within one hour of ATP depletion (and within 15 minutes of recovery) was observed in the current study, and SOD1 over-expression but not MitoTEMPO treatment tended to decrease JNK phosphorylation in both serum free and ATP-DR conditions. SOD1 over-expression also prevented c-Jun phosphorylation, the downstream effector of JNK demonstrated that the c-Jun pathways is likely modified by cytosolic ROS and plays an active role in the downstream activation of apoptosis. This finding corroborates with previously published reports that over-expression of c-Jun leads to cell death in PC12 cells, which can be inhibited by expression of dominant negative c-Jun [52] and suppression of the JNK-c-Jun signaling cascade protects the kidney against IR-induced apoptosis [53]. It was not entirely surprising that MitoTEMPO failed to prevent either phosphorylation of JNK or c-Jun as these are cytosolic signals, most likely activated by cytosolic ROS and the scavenging of mitochondrial ROS may not have a direct effect on these pathways.

In conclusion, this study shows for the first time that SOD1 over-expression and MitoTEMPO treatment partially preserve mitochondrial membrane integrity and attenuate ATP-DR mediated necrosis and apoptosis by preventing mitochondrial permeability transition and decreasing Bax translocation to mitochondria. Although the exact signaling intermediates that form a link between the cytosolic ROS and mitochondrial membrane permeability are not exactly clear yet, it is possible that either mitochondrial K^+ channels and/or the sodium/calcium exchanger (NCX) play a role in activating these signals [54, 55].

Future studies examining the role of these ion channels and the use of genetic techniques to scavenge mitochondrial ROS in renal IRI are warranted.

Acknowledgments

This work was supported in part by an American Heart Association-Scientist Development Grant (0930326G) and departmental funds to V. Nilakantan and NIH grants to ZJB (P01GM066730 and R01HL034708).

Abbreviations

DPBS	Dulbecco's phosphate buffered saline
EGFP	enhance green fluorescent protein
ROS	reactive oxygen species
SOD	superoxide dismutase

References

1. Venkatachalam MA, Jones DB, Rennke HG, Sandstrom D, Patel Y. Mechanism of proximal tubule brush border loss and regeneration following mild renal ischemia. Lab Invest. 1981; 45:355–365. [PubMed: 7300248]
2. Molitoris BA. Ischemia-induced loss of epithelial polarity: potential role of the actin cytoskeleton. Am J Physiol. 1991; 260:F769–F778. [PubMed: 2058700]
3. Kellerman PS, Bogusky RT. Microfilament disruption occurs very early in ischemic proximal tubule cell injury. Kidney Int. 1992; 42:896–902. [PubMed: 1453583]
4. Davies SJ, Reichardt-Pascal SY, Vaughan D, Russell GI. Differential effect of ischaemia-reperfusion injury on anti-oxidant enzyme activity in the rat kidney. Exp Nephrol. 1995; 3:348–354. [PubMed: 8528679]
5. Jassem W, Fuggle SV, Rela M, Koo DD, Heaton ND. The role of mitochondria in ischemia/reperfusion injury. Transplantation. 2002; 73:493–499. [PubMed: 11889418]
6. Weight SC, Bell PR, Nicholson ML. Renal ischaemia--reperfusion injury. Br J Surg. 1996; 83:162–170. [PubMed: 8689154]
7. Nath KA, Norby SM. Reactive oxygen species and acute renal failure. Am J Med. 2000; 109:665–678. [PubMed: 11099687]
8. Lameire N, Vanholder R. Pathophysiologic features and prevention of human and experimental acute tubular necrosis. J Am Soc Nephrol. 2001; 17(12 Suppl):S20–S32. [PubMed: 11251028]
9. Fridovich I. Superoxide radical and superoxide dismutases. Annu Rev Biochem. 1995; 64:97–112. [PubMed: 7574505]
10. Yin M, Wheeler MD, Connor HD, Zhong Z, Bunzendahl H, Dikalova A, Samulski RJ, Schoonhoven R, Mason RP, Swenberg JA, Thurman RG. Cu/Zn-superoxide dismutase gene attenuates ischemia-reperfusion injury in the rat kidney. J Am Soc Nephrol. 2001; 12:2691–2700. [PubMed: 11729238]
11. Chen Z, Siu B, Ho YS, Vincent R, Chua CC, Hamdy RC, Chua BH. Overexpression of MnSOD protects against myocardial ischemia/reperfusion injury in transgenic mice. J Mol Cell Cardiol. 1998; 30:2281–2289. [PubMed: 9925365]
12. Cruthirds DL, Saba H, MacMillan-Crow LA. Overexpression of manganese superoxide dismutase protects against ATP depletion-mediated cell death of proximal tubule cells. Arch Biochem Biophys. 2005; 437:96–105. [PubMed: 15820221]
13. Xiang N, Zhao R, Zhong W. Sodium selenite induces apoptosis by generation of superoxide via the mitochondrial-dependent pathway in human prostate cancer cells. Cancer Chemother Pharmacol. 2009; 63:351–362. [PubMed: 18379781]
14. Burke TJ, Wilson DR, Levi M, Gordon JA, Arnold PE, Schrier RW. Role of mitochondria in ischemic acute renal failure. Clin Exp Dial Apheresis. 1983; 7:49–61. [PubMed: 6883804]

15. Crompton M. The mitochondrial permeability transition pore and its role in cell death. Biochem J. 1999; 341((Pt 2)):233–249. [PubMed: 10393078]
16. Halestrap AP. Mitochondrial calcium in health and disease. Biochim Biophys Acta. 2009; 1787:1289–1290. [PubMed: 19695375]
17. Di Lisa F, Menabo R, Canton M, Barile M, Bernardi P. Opening of the mitochondrial permeability transition pore causes depletion of mitochondrial and cytosolic NAD+ and is a causative event in the death of myocytes in postischemic reperfusion of the heart. J Biol Chem. 2001; 276:2571–2575. [PubMed: 11073947]
18. Duchen MR, Smith PA, Ashcroft FM. Substrate-dependent changes in mitochondrial function, intracellular free calcium concentration and membrane channels in pancreatic beta-cells. Biochem J. 1993; 294((Pt 1)):35–42. [PubMed: 8363584]
19. Liang HL, Arsenault J, Mortensen J, Park F, Johnson CP, Nilakantan V. Partial attenuation of cytotoxicity and apoptosis by SOD1 in ischemic renal epithelial cells. Apoptosis. 2009; 14:1176–1189. [PubMed: 19685188]
20. Nilakantan V, Liang H, Maenpaa CJ, Johnson CP. Differential patterns of peroxynitrite mediated apoptosis in proximal tubular epithelial cells following ATP depletion recovery. Apoptosis. 2008; 13:621–633. [PubMed: 18357533]
21. Nilakantan V, Maenpaa C, Jia G, Roman RJ, Park F. 20-HETE-mediated cytotoxicity and apoptosis in ischemic kidney epithelial cells. Am J Physiol Renal Physiol. 2008; 294:F562–F570. [PubMed: 18171997]
22. Trollinger DR, Cascio WE, Lemasters JJ. Mitochondrial calcium transients in adult rabbit cardiac myocytes: inhibition by ruthenium red and artifacts caused by lysosomal loading of Ca(2+)-indicating fluorophores. Biophys J. 2000; 79:39–50. [PubMed: 10866936]
23. Halestrap AP, Doran E, Gillespie JP, O'Toole A. Mitochondria and cell death. Biochem Soc Trans. 2000; 28:170–177. [PubMed: 10816121]
24. Nakagawa T, Shimizu S, Watanabe T, Yamaguchi O, Otsu K, Yamagata H, Inohara H, Kubo T, Tsujimoto Y. Cyclophilin D-dependent mitochondrial permeability transition regulates some necrotic but not apoptotic cell death. Nature. 2005; 434:652–658. [PubMed: 15800626]
25. Halestrap AP, Clarke SJ, Javadov SA. Mitochondrial permeability transition pore opening during myocardial reperfusion--a target for cardioprotection. Cardiovasc Res. 2004; 61:372–385. [PubMed: 14962470]
26. Devalaraja-Narashimha K, Diener AM, Padanilam BJ. Cyclophilin D gene ablation protects mice from ischemic renal injury. Am J Physiol Renal Physiol. 2009; 297:F749–F759. [PubMed: 19553348]
27. Madesh M, Antonsson B, Srinivasula SM, Alnemri ES, Hajnoczky G. Rapid kinetics of tBid-induced cytochrome c and Smac/DIABLO release and mitochondrial depolarization. J Biol Chem. 2002; 277:5651–5659. [PubMed: 11741882]
28. Tsuruta F, Sunayama J, Mori Y, Hattori S, Shimizu S, Tsujimoto Y, Yoshioka K, Masuyama N, Gotoh Y. JNK promotes Bax translocation to mitochondria through phosphorylation of 14-3-3 proteins. Embo J. 2004; 23:1889–1899. [PubMed: 15071501]
29. Bernardi P, Vassanelli S, Veronese P, Colonna R, Szabo I, Zoratti M. Modulation of the mitochondrial permeability transition pore. Effect of protons and divalent cations. J Biol Chem. 1992; 267:2934–2939. [PubMed: 1737749]
30. Wilson DR, Arnold PE, Burke TJ, Schrier RW. Mitochondrial calcium accumulation and respiration in ischemic acute renal failure in the rat. Kidney Int. 1984; 25:519–526. [PubMed: 6737843]
31. Nguyen KT, Garcia-Chacon LE, Barrett JN, Barrett EF, David G. The Psi(m) depolarization that accompanies mitochondrial Ca2+ uptake is greater in mutant SOD1 than in wild-type mouse motor terminals. Proc Natl Acad Sci U S A. 2009; 106:2007–2011. [PubMed: 19174508]
32. Zhou J, Yi J, Fu R, Liu E, Siddique T, Rios E, Deng HX. Hyperactive intracellular calcium signaling associated with localized mitochondrial defects in skeletal muscle of an animal model of amyotrophic lateral sclerosis. J Biol Chem. 285:705–712. [PubMed: 19889637]
33. Zima AV, Blatter LA. Redox regulation of cardiac calcium channels and transporters. Cardiovasc Res. 2006; 71:310–321. [PubMed: 16581043]

34. Halestrap AP, McStay GP, Clarke SJ. The permeability transition pore complex: another view. Biochimie. 2002; 84:153–166. [PubMed: 12022946]
35. Zorov DB, Filburn CR, Klotz LO, Zweier JL, Sollott SJ. Reactive oxygen species (ROS)-induced ROS release: a new phenomenon accompanying induction of the mitochondrial permeability transition in cardiac myocytes. J Exp Med. 2000; 192:1001–1014. [PubMed: 11015441]
36. Liu Y, Borchert GL, Donald SP, Surazynski A, Hu CA, Weydert CJ, Oberley LW, Phang JM. MnSOD inhibits proline oxidase-induced apoptosis in colorectal cancer cells. Carcinogenesis. 2005; 26:1335–1342. [PubMed: 15817612]
37. Tauskela JS. MitoQ--a mitochondria-targeted antioxidant. IDrugs. 2007; 10:399–412. [PubMed: 17642004]
38. Adlam VJ, Harrison JC, Porteous CM, James AM, Smith RA, Murphy MP, Sammut IA. Targeting an antioxidant to mitochondria decreases cardiac ischemia-reperfusion injury. Faseb J. 2005; 19:1088–1095. [PubMed: 15985532]
39. Supinski GS, Murphy MP, Callahan LA. MitoQ administration prevents endotoxin-induced cardiac dysfunction. Am J Physiol Regul Integr Comp Physiol. 2009; 297:R1095–R1102. [PubMed: 19657095]
40. Graham D, Huynh NN, Hamilton CA, Beattie E, Smith RA, Cocheme HM, Murphy MP, Dominiczak AF. Mitochondria-targeted antioxidant MitoQ10 improves endothelial function and attenuates cardiac hypertrophy. Hypertension. 2009; 54:322–328. [PubMed: 19581509]
41. Green DR, Reed JC. Mitochondria and apoptosis. Science. 1998; 281:1309–1312. [PubMed: 9721092]
42. Antonsson B, Montessuit S, Lauper S, Eskes R, Martinou JC. Bax oligomerization is required for channel-forming activity in liposomes and to trigger cytochrome c release from mitochondria. Biochem J. 2000; 345(Pt 2):271–278. [PubMed: 10620504]
43. Halestrap AP. Mitochondria and reperfusion injury of the heart--a holey death but not beyond salvation. J Bioenerg Biomembr. 2009; 41:113–121. [PubMed: 19357938]
44. Lin CH, Lu YZ, Cheng FC, Chu LF, Hsueh CM. Bax-regulated mitochondria-mediated apoptosis is responsible for the in vitro ischemia induced neuronal cell death of Sprague Dawley rat. Neurosci Lett. 2005; 387:22–27. [PubMed: 16084019]
45. Fujimura M, Morita-Fujimura Y, Narasimhan P, Copin JC, Kawase M, Chan PH. Copper-zinc superoxide dismutase prevents the early decrease of apurinic/apyrimidinic endonuclease and subsequent DNA fragmentation after transient focal cerebral ischemia in mice. Stroke. 1999; 30:2408–2415. [PubMed: 10548678]
46. Fujimura M, Morita-Fujimura Y, Noshita N, Sugawara T, Kawase M, Chan PH. The cytosolic antioxidant copper/zinc-superoxide dismutase prevents the early release of mitochondrial cytochrome c in ischemic brain after transient focal cerebral ischemia in mice. J Neurosci. 2000; 20:2817–2824. [PubMed: 10751433]
47. Saito A, Hayashi T, Okuno S, Nishi T, Chan PH. Oxidative stress is associated with XIAP and Smac/DIABLO signaling pathways in mouse brains after transient focal cerebral ischemia. Stroke. 2004; 35:1443–1448. [PubMed: 15118177]
48. Fu YC, Yin SC, Chi CS, Hwang B, Hsu SL. Norepinephrine induces apoptosis in neonatal rat endothelial cells via a ROS-dependent JNK activation pathway. Apoptosis. 2006; 11:2053–2063. [PubMed: 17041759]
49. Kim J, Sharma RP. Calcium-mediated activation of c-Jun NH2-terminal kinase (JNK) and apoptosis in response to cadmium in murine macrophages. Toxicol Sci. 2004; 81:518–527. [PubMed: 15254339]
50. Murakami T, Takagi H, Suzuma K, Suzuma I, Ohashi H, Watanabe D, Ojima T, Suganami E, Kurimoto M, Kaneto H, Honda Y, Yoshimura N. Angiopoietin-1 attenuates H2O2-induced SEK1/JNK phosphorylation through the phosphatidylinositol 3-kinase/Akt pathway in vascular endothelial cells. J Biol Chem. 2005; 280:31841–31849. [PubMed: 16000309]
51. Suzuma I, Murakami T, Suzuma K, Kaneto H, Watanabe D, Ojima T, Honda Y, Takagi H, Yoshimura N. Cyclic stretch-induced reactive oxygen species generation enhances apoptosis in retinal pericytes through c-jun NH2-terminal kinase activation. Hypertension. 2007; 49:347–354. [PubMed: 17159082]

52. Ham J, Babij C, Whitfield J, Pfarr CM, Lallemand D, Yaniv M, Rubin LL. A c-Jun dominant negative mutant protects sympathetic neurons against programmed cell death. Neuron. 1995; 14:927–939. [PubMed: 7748560]

53. Wang Y, Ji HX, Xing SH, Pei DS, Guan QH. SP600125, a selective JNK inhibitor, protects ischemic renal injury via suppressing the extrinsic pathways of apoptosis. Life Sci. 2007; 80:2067–2075. [PubMed: 17459422]

54. Eigel BN, Gursahani H, Hadley RW. Na+/Ca2+ exchanger plays a key role in inducing apoptosis after hypoxia in cultured guinea pig ventricular myocytes. Am J Physiol Heart Circ Physiol. 2004; 287:H1466–H1475. [PubMed: 15155263]

55. Eigel BN, Gursahani H, Hadley RW. ROS are required for rapid reactivation of Na+/Ca2+ exchanger in hypoxic reoxygenated guinea pig ventricular myocytes. Am J Physiol Heart Circ Physiol. 2004; 286:H955–H963. [PubMed: 14592940]

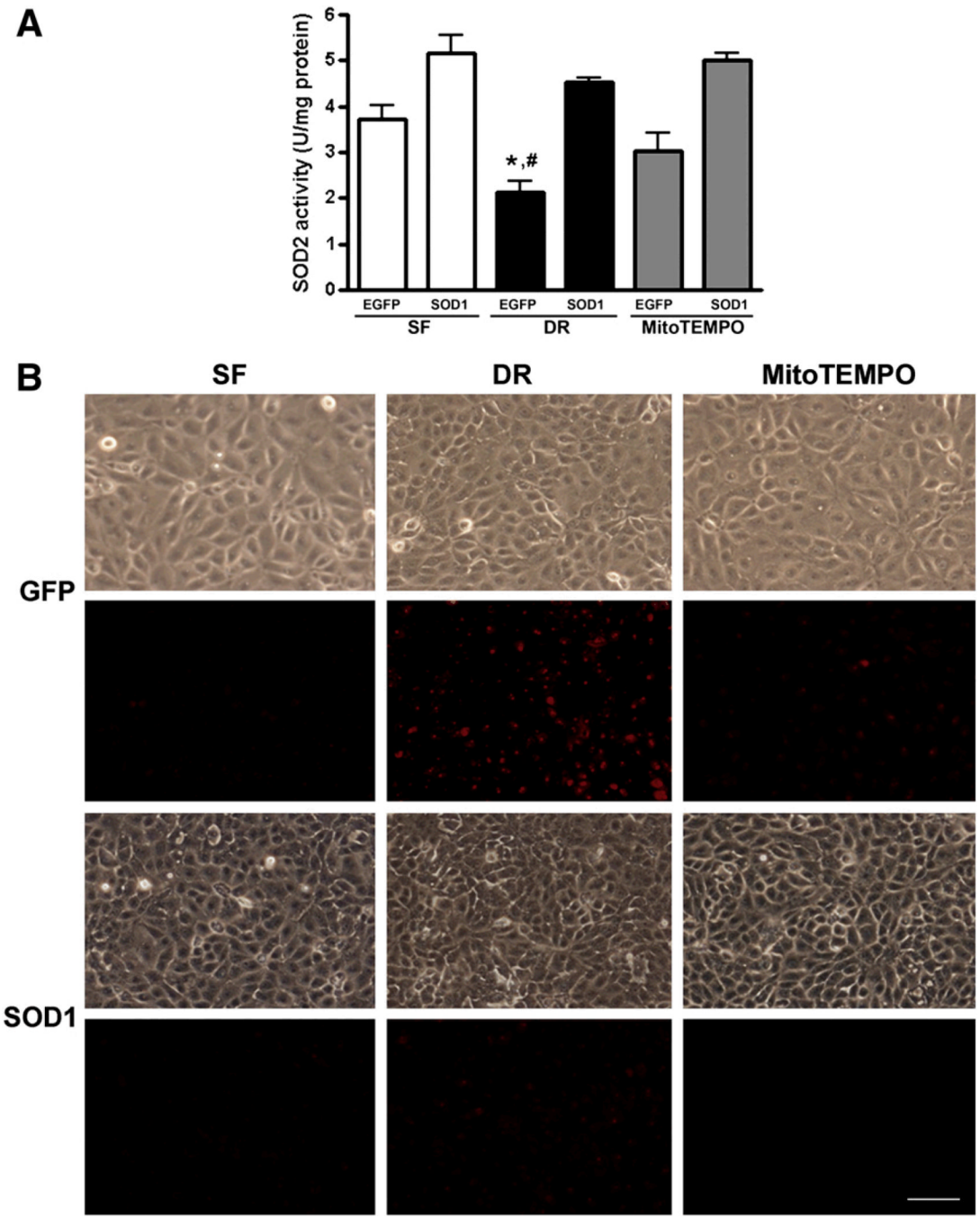

Fig. 1.

A: SOD2 activity in EGFP, SOD1 and MitoTEMPO treated cells under serum free and 2h-1h ATP-DR conditions. Results are means ± SEM. N=3 per group. * P<0.05 vs. EGFP-SF; # P<0.01 vs. EGFP-MitoTEMPO. B: Light and DHE fluorescent images in EGFP, SOD1 and MitoTEMPO treated cells under serum free and 2h-1h ATP-DR conditions. Scale bar = 60 μm.

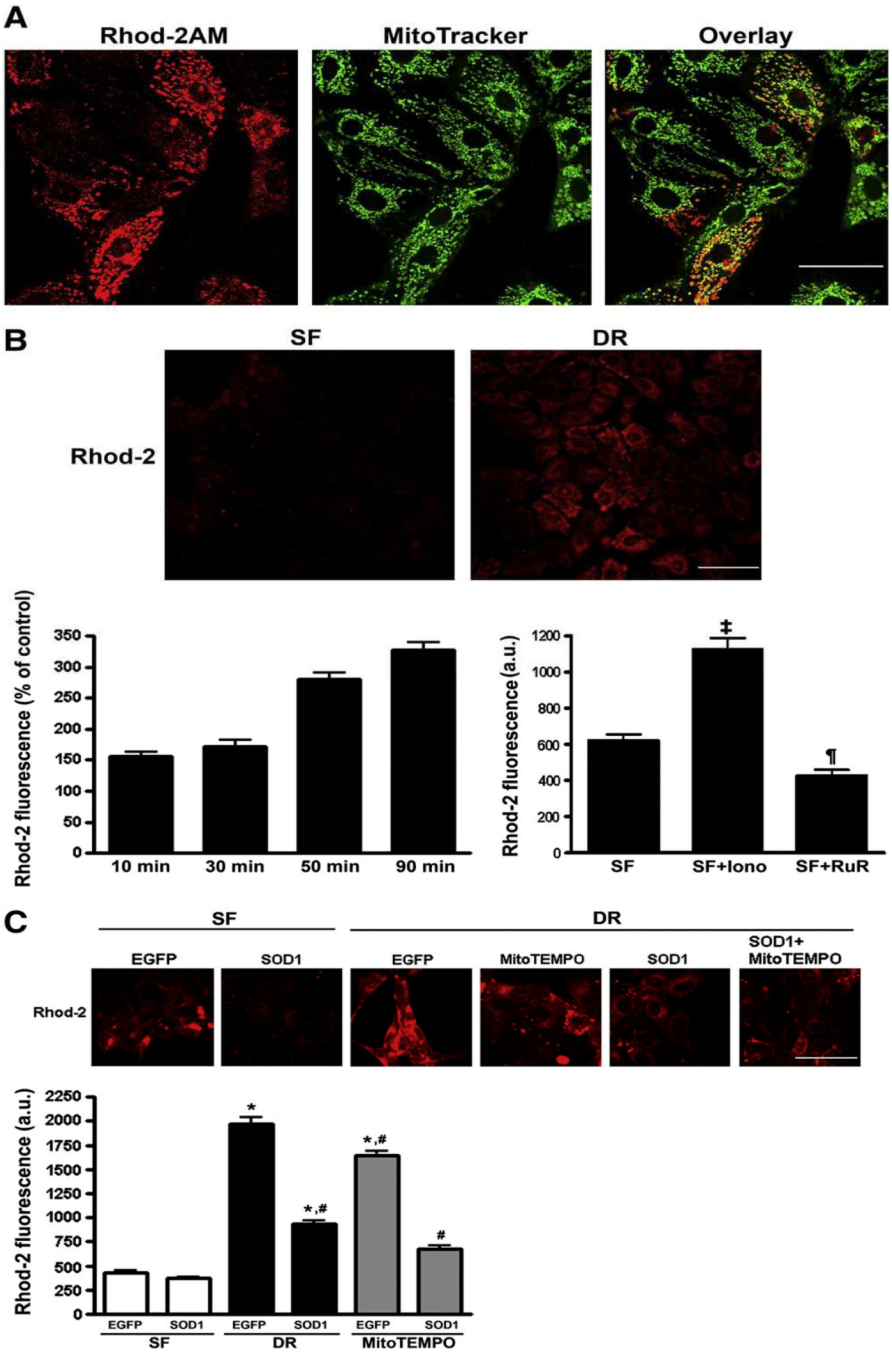

Fig. 2.

A: Co-localization of rhod-2 and MitoTracker fluorescence in LLC-PK$_1$ cells. B: Time course of rhod-2 fluorescence following 1 h ATP depletion and varying recovery times indicates progressive accumulation of mitochondrial Ca^{2+}. Ca^{2+} ionophore, ionomycin increases mitochondrial Ca^{2+}, which is blocked by inhibiting mitochondrial Ca^{2+} uptake with ruthenium red. ¶, $P < 0.01$ Ruthenium vs. serum free (SF); ‡, $P < 0.001$ Ionomycin vs. SF. C: Representative images (top panel) and summary histograms of rhod-2 fluorescence intensity (bottom bar graph) in LLC-EGEP and LLC-SOD1 cells following 1h-1h ATP depletion- recovery. Results are means ± SEM, with N=80–100 cells from 4 different dishes.

*, P < 0.05 vs. SF; #, P < 0.05 vs. EGFP-DR. Scale bar = 25 μm for 1A, 40 μm for 1B and 1C.

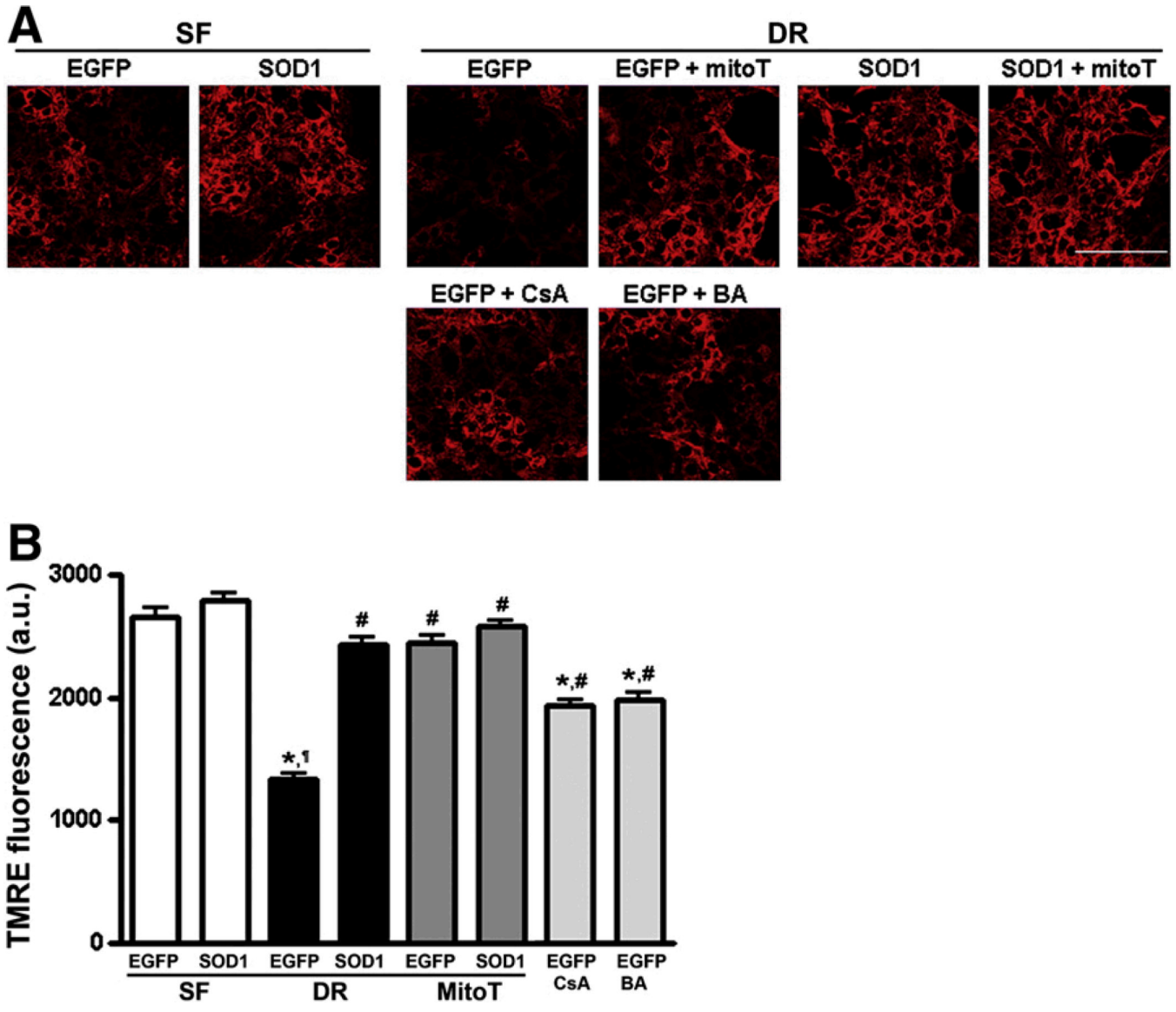

Fig. 3.

SOD1 over-expression and MitoTEMPO attenuate the loss of $\Delta\Psi_m$ due to MPTP opening. $\Delta\Psi_m$ was assayed by TMRE fluorescence in LLC-SOD1 and LLC-EGFP cells with or without MitoTEMPO after 1h-1h ATP-DR. A: Representative images. B: Summary histograms of TMRE fluorescence intensity. ATP depletion recovery causes complete dissipation of $\Delta\Psi_m$ (DR, EGFP) which is prevented by MPTP inhibition with cyclosporine A (CsA) or bongkrekic acid (BA). ROS scavenging by SOD1 or MitoTEMPO also attenuated the loss of $\Delta\Psi_m$. Results are means ± SEM, with N=80–100 cells from 4 different dishes. * $P < 0.01$ vs. SF; #, $P < 0.05$ vs. SF. ¶ $P<0.001$ EGFP-DR vs. all other groups. Scale bar = 50 μm.

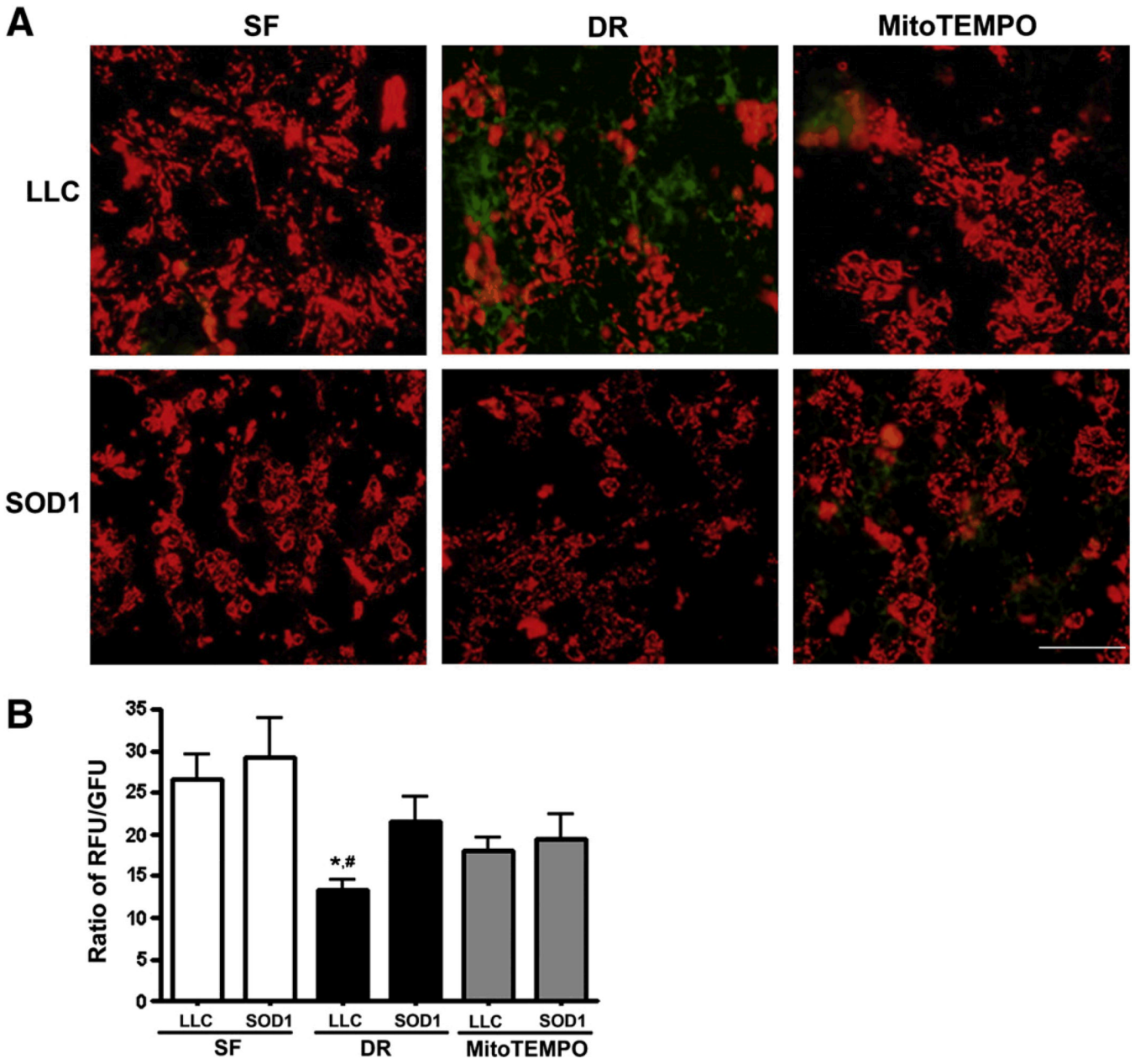

Fig. 4.

SOD1 over-expression and MitoTEMPO prevent the loss of loss of $\Delta\Psi_m$ as measured by JC-1. As in Fig 2, cells were exposed to 1h-1h ATP-DR A: Representative JC-1 images of LLC-PK_1 (top panel) and LLC-SOD1 (low panel) cells. B: Quantitation of JC-1 fluorescence. Results are ratios of red to green JC-1 fluorescence and presented as means ± SEM (N=9 for all groups). * $P < 0.05$ vs. SOD1-DR; #, $P < 0.01$ vs. SF. Scale bar = 40 μm.

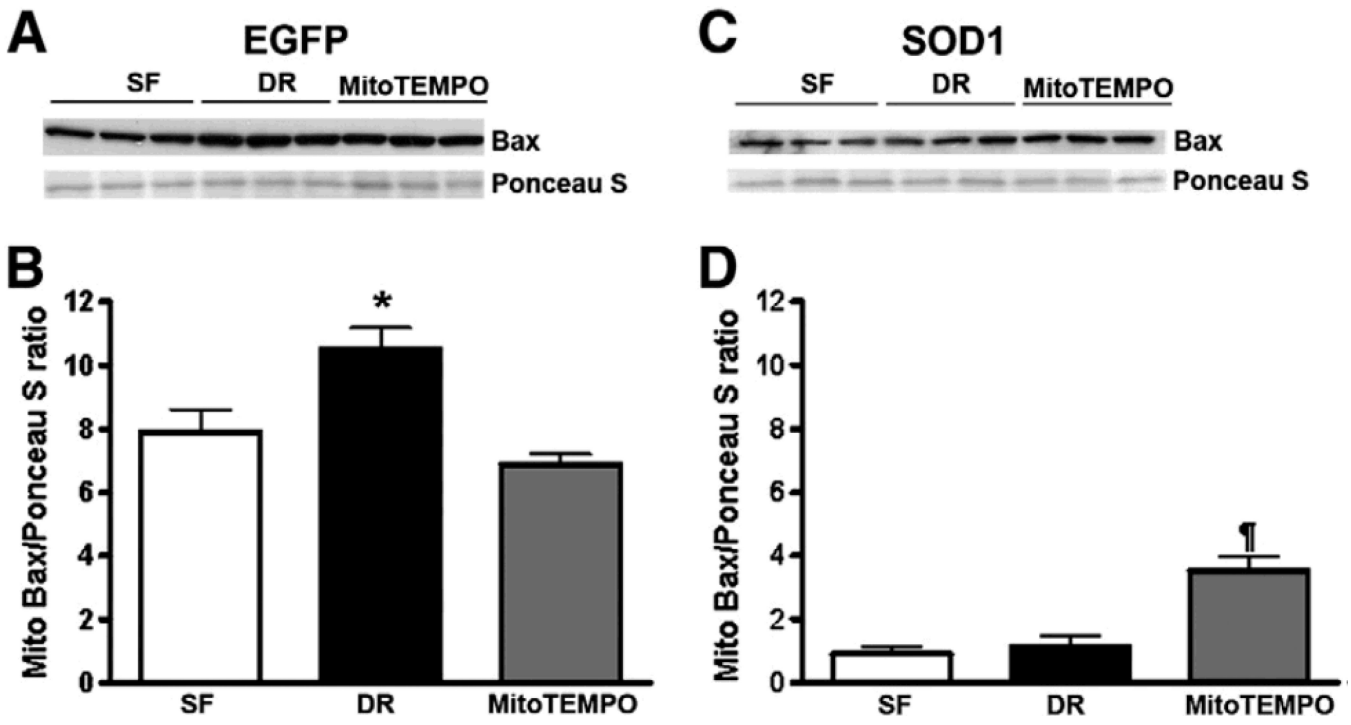

Fig. 5.

Densitometry of Bax western blots in mitochondrial fraction from LLC-SOD1and LLC-EGFP cells following 1h-1h ATP-DR (DR) with or without MitoTEMPO (MitoTEMPO). Serum free (SF) cells were used as control. A: western blot of Bax in EGFP cells with Ponceau S as loading control; C: western blot of Bax in SOD1 cells with Ponceau S as loading control. B and D: Densitometry ratio of Bax to Ponceau S staining. Over-expression of SOD1 prevents Bax translocation to mitochondria. Results are means ± SEM. N=3; * $P < 0.05$ EGFP-DR vs. SF and MitoTEMPO; ¶, $P < 0.01$, SOD1-MitoTEMPO vs. SF and SOD1-DR.

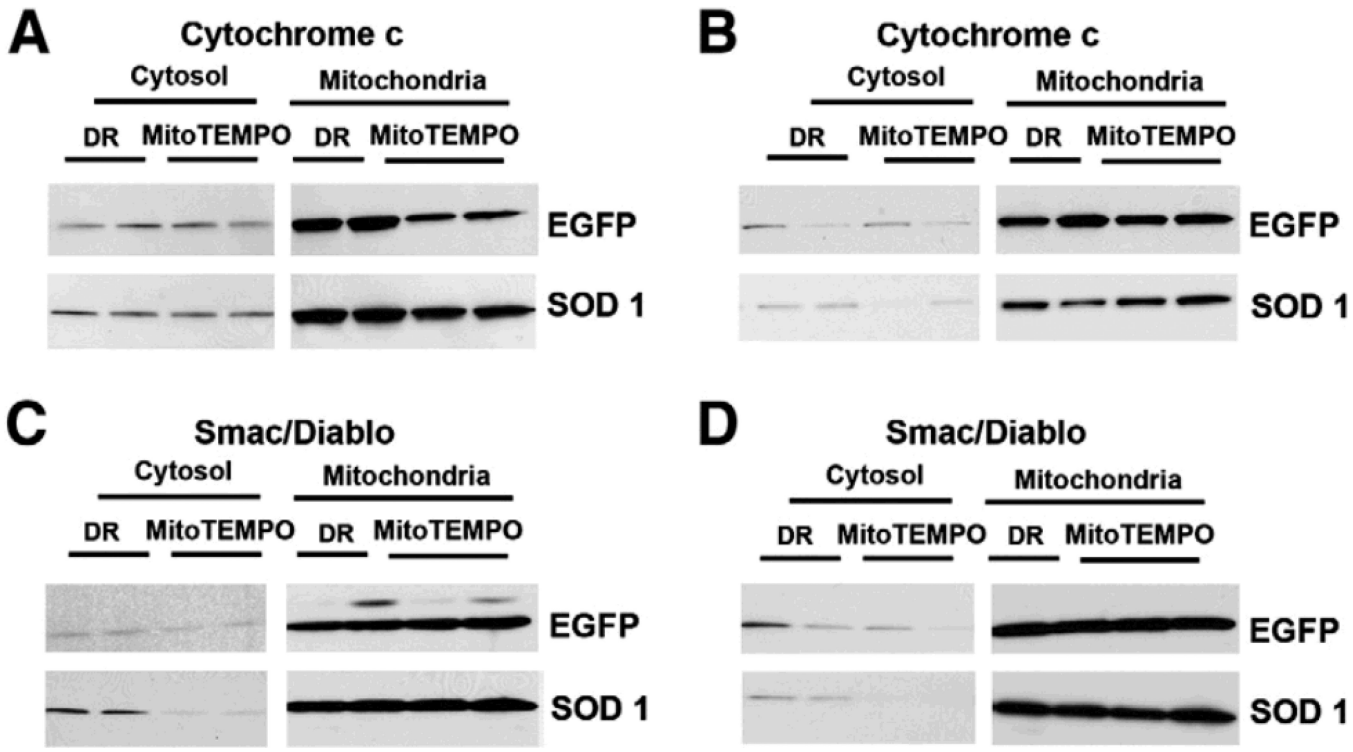

Fig. 6.

Western blots of cytochrome *c* (A and B) and Smac/Diablo (C and D) in mitochondrial and cytosol fraction in both EGFP and SOD1 cells with or without MitoTEMPO following 1h-1h or 2h-1h ATP-DR. A: Western blot from 1h-1h: cytochrome *c* in cytosol fraction (left panel), cytochrome *c* in mitochondrial fraction (right panel). B: Western blot from 2h-1h protocol: cytochrome *c* in cytosol fraction (left panel), cytochrome *c* in mitochondrial fraction (right panel).C: Western Blot of 1h-1h ATP-DR: Smac/Diablo in cytosolic fraction (left panel), Smac/Diablo in mitochondrial fraction (right panel). B: Western Blot of 2h-1h ATP-DR: Smac/Diablo in cytosol fraction (left panel), Smac/Diablo in mitochondrial fraction (right panel).

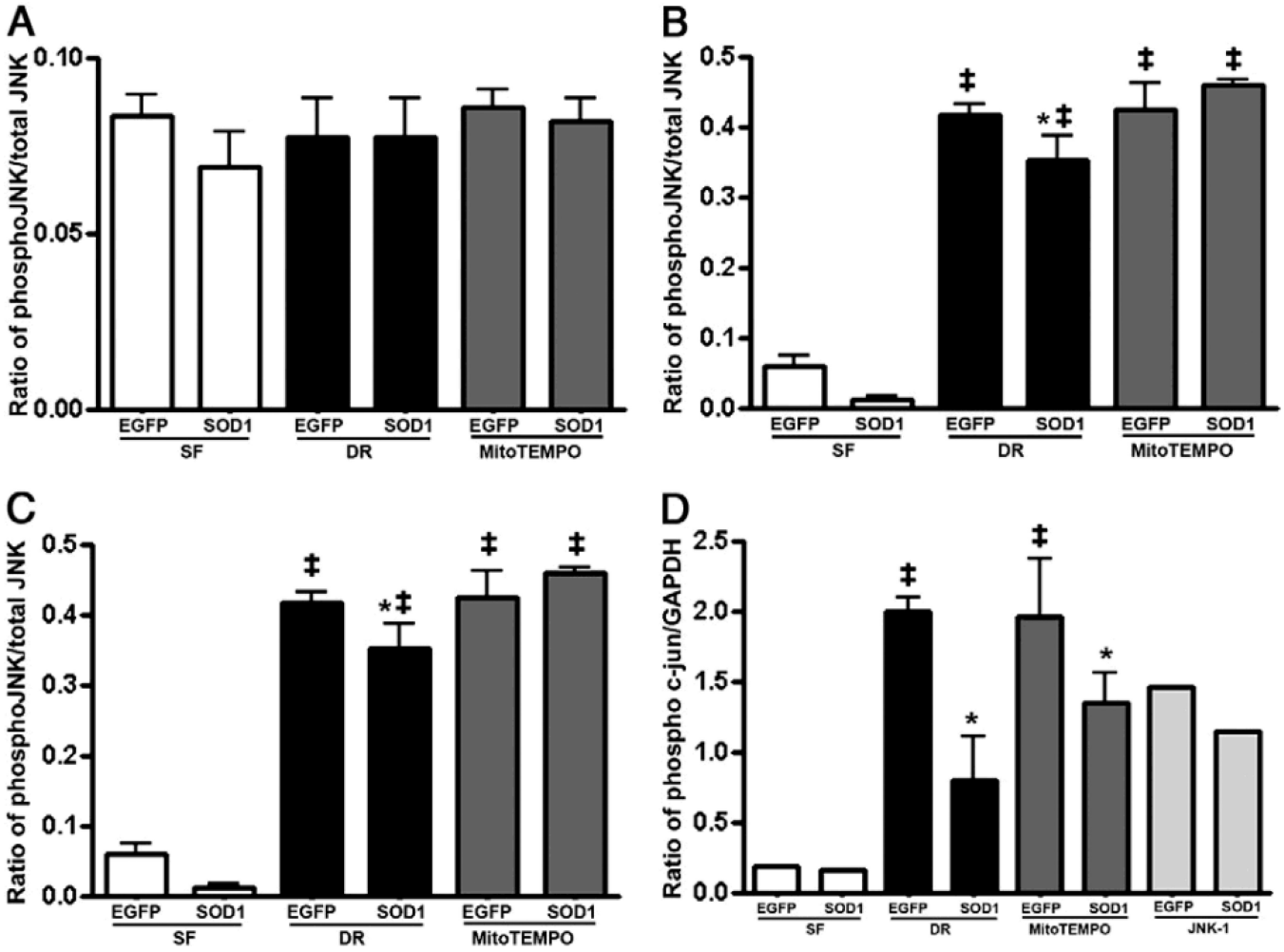

Fig. 7.

Densitometry of pJNK and phospho-c-Jun western blots in whole cell lysate from LLC-SOD1and LLC-EGFP cells following different time points of ATP-DR with or without MitoTEMPO. A-C: Densitometry ratio of pJNK to total JNK in 30 min-5 min, 1h-15 min, and 2h-30 min. Over-expression of SOD1 prevents JNK phosphorylation in 1h or 2h ATP-DR but no effect at the 30 min ischemic time point. Results are means ± SEM. N=3; ‡, $P < 0.001$ vs. SF. D: Densitometry ratio of phospho-c-Jun to GAPDH. SOD1 also prevents c-Jun phosphorylation following 1h-15 min of ATP-DR. MitoTEMPO did not show any changes in either JNK or c-Jun phosphorylation. ‡, $P<0.01$ vs. SF; *, $P < 0.05$ vs. EGFP-DR.

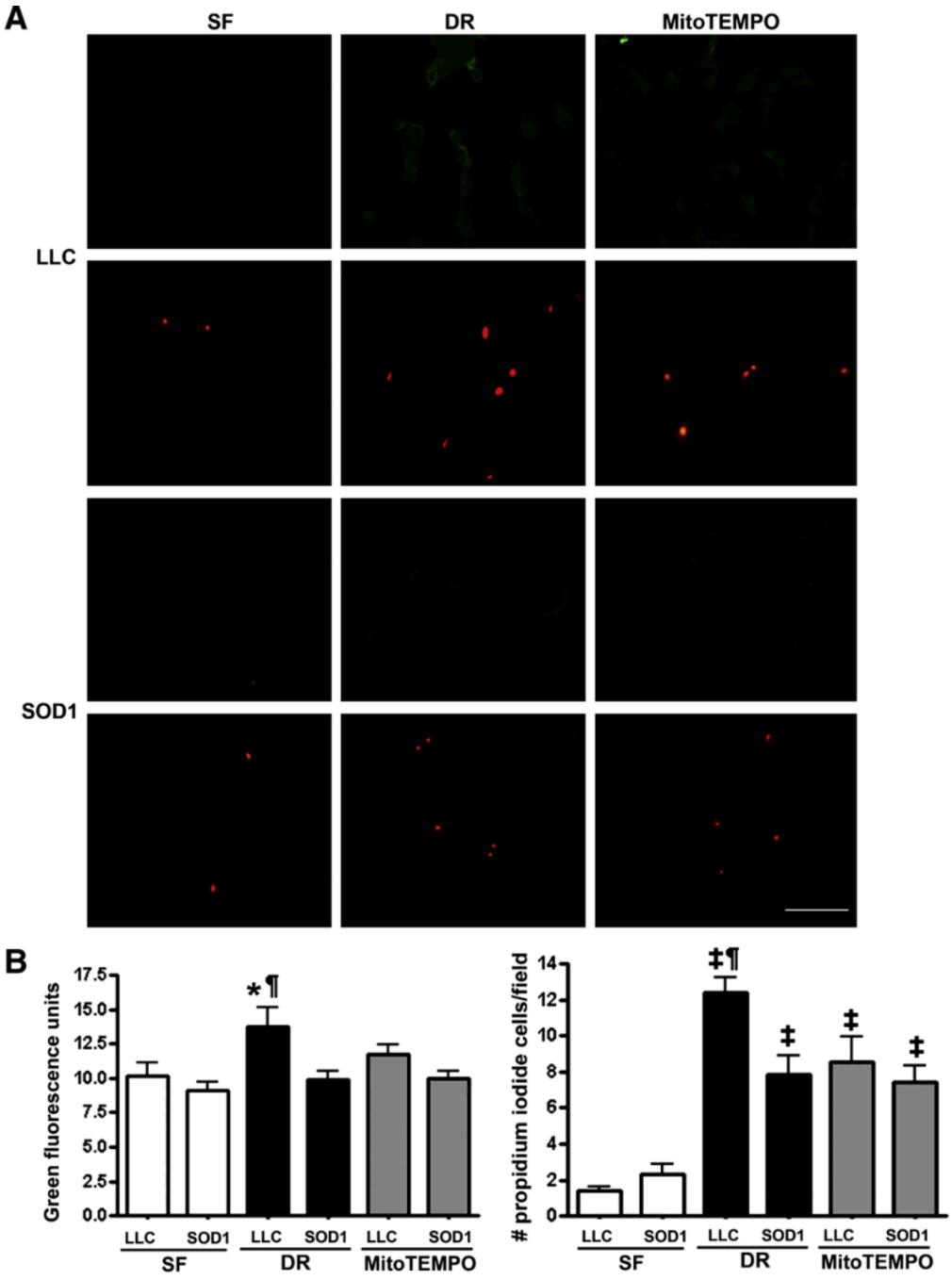

Fig. 8.

Annexin V and propidium staining in LLC-SOD1 and LLC-PK$_1$ cells with or without MitoTEMPO following 2h-1h ATP-DR. A: Annexin V and propidium staining in LLC-PK$_1$ (top panel) and LLC-SOD1 (lower panel). B: Quantitation of Annexin V fluorescence. C: The number of propidium iodide positive cells per field. SOD1 and MitoTEMPO significantly reduced Annexin V green fluorescence and the percentage of propidium positive cells. N=5–12; *, $P < 0.05$, LLC-DR vs. SOD-DR, SF, SOD-MitoTEMPO; ¶, $P < 0.01$, LLC-DR vs. SOD-MitoTEMPO; ‡, $P < 0.001$vs. SF. Scale bar = 60 μm.